Circuit synthesizable Guaranteed Passive Modeling for *Multiport* Structures

Zohaib Mahmood
Massachusetts Institute of Technology
zohaib@mit.edu

Luca Daniel
Massachusetts Institute of Technology
luca@mit.edu

ABSTRACT

In this paper we present a highly efficient algorithm to automatically generate *circuit synthesizable* dynamical models for *passive* multiport structures. The algorithm is based on a natural convex relaxation of the original nonconvex problem of modeling multiport devices from frequency response data, subject to global passivity constraints. The algorithm identifies a collection of first and second order passive networks interconnected in either series or parallel fashion. Passive models for several multiport structures, including wilkinson type combiner, power grid and coupled on-chip inductors are provided to corroborate the theoretical development and show efficacy of the implemented algorithm. To demonstrate the full strength of our algorithm, the identified models are also interfaced with commercial simulators and used to perform time domain simulations while being connected to highly nonlinear power amplifiers.

1. INTRODUCTION

Automatic generation of accurate, compact and passive dynamical models for multiport passive interconnect structures from frequency response is a crucial part of the design flow for complex analog systems. Typically, passive structures are simulated by a field solver which computes frequency response data samples in the desired frequency band. Based on the frequency response samples extracted by the solver or collected from measurements, a reduced model is developed which can be incorporated into a circuit simulator for time domain simulations of a larger system containing also nonlinear devices. A model violating any basic physical property, such as passivity, can cause convergence issues for the simulator, huge errors in the response of the overall system, and the results may become completely nonphysical.

There exist different approaches to generate dynamical models from frequency response data. The problem of finding a passive multiport model from complex frequency response data is highly nonlinear and non convex. Given a set of frequency response samples $\{H_i, \omega_i\}$, where $H_i = H(j\omega_i)$ are the transfer matrix samples of some unknown multiport linear system, the compact modeling task is to construct a low-order rational transfer matrix $\hat{H}(s)$ such that $\hat{H}(j\omega_i) \approx H_i$. Formulated as an L_2 minimization problem of the sum of squared errors, it can be written as (1)

$$\begin{aligned} \underset{\hat{H}}{\text{minimize}} \quad & \sum_i \left| H_i - \hat{H}(j\omega_i) \right|^2 \\ \text{subject to} \quad & \hat{H}(j\omega) \quad \textit{passive} \end{aligned} \tag{1}$$

Even after ignoring the passivity constraint in (1), the unconstrained minimization problem is non-convex and is therefore very difficult to solve. Direct solution using nonlinear least squares have been proposed, such as Lavenberg-Marquardt [1]. There is no guarantee that such approach will converge to the global minimum, and quite often the algorithm will yield only a locally optimal result. Over the past years considerable effort has been put into finding a convex relaxation to the original problem, several published exists such as [2–4]. Although these techniques provide a solid theoretical framework and analytical formulation, they are often criticized as being computationally expensive. Most of these techniques rely on enforcing some formulation of the positive real lemma by constraining the real part of the impedance matrix to be positive definite over *all frequencies*. Although such a constraint can be certifiably enforced by using Sum-Of-Squares (*SOS*) relaxation, it is normally a costly operation, specially when the constraints are defined on frequency dependent matrices such as in [3, 4].

Some heuristics-based iterative techniques also do exist such as [5, 6]. In these techniques a stable but non-passive model is first identified. This non-passive model is then checked for passivity violations by examining if there exist pure imaginary eigen values of the corresponding Hamiltonian matrix. As the final step, some parameters of the initially identified non-passive model are perturbed to correct for passivity violations. Although these techniques are computationally efficient, however since perturbing the system is an ill-posed problem, there is no guarantee that the final passivated model is optimal for accuracy.

In this paper we present a *theoretical and analytical formulation* and a *highly efficient implementation* of a procedure for identifying passive dynamical models from frequency response data for multiport structures. We solve the problem in two steps, first a set of common poles is identified using already established techniques [3, 7, 8]. Next we identify residue matrices while simultaneously enforcing passivity using frequency independent linear matrix inequalities. Although, similar conditions for passivity were derived in [9, 10], the conditions were used *only* to 'check' for passivity violations as opposed to our proposed algorithm where these conditions are built into the model identification procedure to 'enforce' passivity. Also, no efficient algorithm was proposed in [9, 10] to rectify for passivity violations. For example in [9] it was proposed that the pole-residue pairs violating passivity conditions should be discarded, this is highly restrictive and can significantly deteriorate the accuracy. We instead propose that the identified residue matrices should conform to passivity conditions during the identification such that there are no passivity violation in the final model. The formulation presented in this paper, being convex, is guaranteed to converge to the global minimum and can be easily implemented using publicly available convex optimization solvers such as SeDuMi [11]. Also, since the constraints presented in this paper are frequency independent, for the same model accuracy we get orders of magnitude improvement in terms of speed compared to other convex optimization based techniques such as [3, 4] where the the constraints are frequency dependent and are expensive to enforce. The scheme presented in this paper can potentially be extended to generate parameterized models with apriori global passivity certificate. Finally, the models generated by our algorithm can readily be synthesized into an equivalent passive network and can be interfaced with commercial circuit simulators by generating either a spice-like netlist or a Verilog-A model.

The remainder of the paper is organized as follows: Section 2 describes the rational fitting of transfer matrices and the notion of passivity. Section 3 formulates the problem of passive fitting for multiport LTI systems. Section 4 details the full algorithm for our modeling approach. Finally, Section 5 demonstrates the effectiveness of the proposed approach in modeling various multiport struc-

tures.

2. BACKGROUND

2.1 Rational Transfer Matrix Fitting

The problem of constructing a rational approximation of multi port systems consists of finding residue matrices $\mathbf{R_k}$, poles a_k and the matrices $\mathbf{D}$ & $\mathbf{F}$ such that the identified model, defined by the transfer function $\hat{H}(s)$ in (2), minimizes the mismatch between the reduced model and the original system as described in (1).

$$\hat{H}(s) = \sum_{i=1}^{\kappa} \frac{\mathbf{R_k}}{s - a_k} + \mathbf{D} + s\mathbf{F} \tag{2}$$

where $\mathbf{R_k}, \mathbf{D}$ and $\mathbf{F}$ are $T \times T$ residue matrices (assuming the system has T ports) and a_k are poles. Since most of the passive structures have a symmetric response, $\mathbf{R_k}, \mathbf{D}$ and $\mathbf{F}$ are symmetric matrices.

2.2 Passivity of Immitance [1] Transfer Matrix

Passivity is the inability of a system (or model) to generate energy. Passivity is an essential property if the model being interconnected with other systems is to be used for time domain simulations, since arbitrary connections of passive systems are guaranteed to be passive. While it may be possible for a non-passive model to provide high accuracy in the frequency domain, the same model when used in time domain simulation could produce extremely inaccurate results resulting from passivity violations.

Passivity for an impedance or admittance system corresponds to *'positive realness'* of the transfer matrix. To be *positive real*, the transfer matrix $\hat{H}(s)$ must satisfy the following constraints

$$\overline{\hat{H}(\bar{s})} = \hat{H}(s) \tag{3a}$$

$$\hat{H}(s) \text{ is analytic in } \Re\{s\} > 0 \tag{3b}$$

$$\hat{H}(j\omega) + \hat{H}(j\omega)^{\dagger} \succeq 0 \ \ \forall\omega \tag{3c}$$

Where $\Re\{\ \}$ denotes the real part and $\dagger$ indicates the hermitian transpose.

The first condition (3a), commonly known as *conjugate symmetry*, ensures that the impulse response corresponding to $\hat{H}(s)$ is real. The second condition (3b) implies stability of the transfer function. A causal linear system in the transfer matrix form is stable if all of its poles are in the left half of the complex plane, i.e. all the poles have negative real part. The third and final condition (3c), which is *positivity condition*, implies positive realness of the symmetric part of the transfer matrix on the $j\omega$ axis.

3. PASSIVE FITTING FOR MULTIPORT LTI SYSTEMS

3.1 Problem Formulation

We expand the summation for $\hat{H}(s)$ in (2). Also since we are mainly interested in the properties of $H(s)$ on the imaginary axis, we replace s with $j\omega$.

$$\hat{H}(j\omega) = \sum_{k=1}^{\kappa_r} \frac{\mathbf{R_k^r}}{j\omega - a_k^r} + \sum_{k=1}^{\kappa_c} \frac{\mathbf{R_k^c}}{j\omega - a_k^c} + \mathbf{D} + j\omega\mathbf{F} \tag{4}$$

Where κ_r and κ_c denote the number of purely real and the number of complex poles, respectively. Also, $\mathbf{R_k^r} \in \mathbb{R}^{T\times T}$, $\mathbf{R_k^c} \in \mathbb{C}^{T\times T}$, $a_k^r \in \mathbb{R}$, $a_k^c \in \mathbb{C}\ \forall k$, and $\mathbf{D}, \mathbf{F} \in \mathbb{R}^{T\times T}$, where T is the number of ports. In the following subsections, we consider one by one the implications of each passivity condition in (3) on the structure of (4).

3.2 Conjugate Symmetry

The terms in (4) corresponding to the matrices $\mathbf{D}$ and $\mathbf{F}$, and to the summation over purely real poles satisfy automatically the first passivity condition (3a). On the other hand such condition *requires* that the complex-poles a_k^c and complex residue matrices $\mathbf{R_k^c}$ always come in *complex-conjugate-pairs*. The proof is given in Appendix A.

$$\hat{H}(j\omega) = \sum_{k=1}^{\kappa_r} \frac{\mathbf{R_k^r}}{j\omega - a_k^r} + \sum_{k=1}^{\kappa_c/2} \left\{ \frac{\Re\mathbf{R_k^c} + j\Im\mathbf{R_k^c}}{j\omega - \Re a_k^c - j\Im a_k^c} + \frac{\Re\mathbf{R_k^c} - j\Im\mathbf{R_k^c}}{j\omega - \Re a_k^c + j\Im a_k^c} \right\} + \mathbf{D} + j\omega\mathbf{F} \tag{5}$$

Here $\Re$ and $\Im$ indicate the real and imaginary parts respectively. Note that the summation for complex poles now extends only upto $\kappa_c/2$. Rewritting (5) compactly:

$$\hat{H}(j\omega) = \sum_{k=1}^{\kappa_r} \hat{H}_k^r(j\omega) + \sum_{k=1}^{\kappa_c/2} \hat{H}_k^c(j\omega) + \mathbf{D} + j\omega\mathbf{F} \tag{6}$$

$$\text{where: } \hat{H}_k^r(j\omega) = \frac{\mathbf{R_k^r}}{j\omega - a_k^r} \tag{7}$$

$$\hat{H}_k^c(j\omega) = \frac{\Re\mathbf{R_k^c} + j\Im\mathbf{R_k^c}}{j\omega - \Re a_k^c - j\Im a_k^c} + \frac{\Re\mathbf{R_k^c} - j\Im\mathbf{R_k^c}}{j\omega - \Re a_k^c + j\Im a_k^c} \tag{8}$$

3.3 Stability

The second condition (3b) which requires analyticity of $\hat{H}(s)$ in $\Re\{s\} > 0$ implies stability. For a linear causal system in pole-residue form (2), the system is strictly stable if all of its poles a_k are in the left half of complex plane i.e. they have negative real part ($\Re\{a_k\} < 0$).

3.4 Positivity

The positivity condition for passivity (3c) is the most difficult condition to enforce analytically. We present here an extremely efficient condition which implies (3c). We consider the case when all the building blocks in the summation (6), namely: purely real poles/residues $\hat{H}_k^r(j\omega)$, complex-conjugate pairs of poles/residues $\hat{H}_k^c(j\omega)$, and the direct term matrix D are individually positive real. Please note that the $j\omega\mathbf{F}$ term has purely imaginary response and therefore does not affect positivity condition.

LEMMA 3.1. (Positive Real Summation Theorem) *Let $\hat{H}(j\omega)$ be a stable and conjugate symmetric transfer matrix given by* (6)*, then $\hat{H}(j\omega)$ is positive-real if $\hat{H}_k^r(j\omega)$, $\hat{H}_k^c(j\omega)$ and D are positive-real $\forall k$. i.e.*

$$\Re\hat{H}_k^r(j\omega) \succeq 0, \Re\hat{H}_k^c(j\omega) \succeq 0 \forall k \ \&\ D \succeq 0 \implies \hat{H}(j\omega) \succeq 0 \tag{9}$$

PROOF. The sum of positive-real, complex matrices is positive real. □

Lemma 3.1 describes a *sufficient*, but *not-necessary*, condition for (3c). In the following subsections we derive the equivalent conditions of positive realness on each term separately.

3.4.1 Purely Real Pole-Residues

In this section we derive the condition for the purely real pole/residue term $\hat{H}_k^r(j\omega)$ in the summation (6) to be positive real. Such a condition can be obtained by rationalizing $\hat{H}_k^r(j\omega)$ as in (7), which results into:

$$\hat{H}_k^r(j\omega) = -\frac{a_k^r\mathbf{R_k^r}}{\omega^2 + {a_k^r}^2} - j\frac{\omega\mathbf{R_k^r}}{\omega^2 + {a_k^r}^2} \tag{10}$$

$$\Re\hat{H}_k^r(j\omega) \succeq 0 \implies -\frac{a_k^r\mathbf{R_k^r}}{\omega^2 + {a_k^r}^2} \succeq 0\ \forall\omega, k = 1, ..., \kappa_r \tag{11}$$

3.4.2 Complex Conjugate Pole-Residues

In this section we derive the positive realness condition for the complex pole/residue term $\hat{H}_k^c(j\omega)$ in the summation (6). Since complex terms always appear conjugate pairs, we first add the two terms for $\hat{H}_k^c(j\omega)$ in (8) resulting into:

$$\hat{H}_k^c(j\omega) = \frac{-2(\Re a_k^c)(\Re\mathbf{R_k^c}) - 2(\Im a_k^c)(\Im\mathbf{R_k^c}) + j2\omega(\Re\mathbf{R_k^c})}{(\Re a_k^c)^2 + (\Im a_k^c)^2 - \omega^2 - j2\omega\Re a_k^c} \tag{12}$$

[1] The term **Immitance** refers to **Im**pedance and Ad**mitance** collectively.

$$\hat{H}_k^c(j\omega) = \frac{-2\{(\Re a_k^c)^3 + \Re a_k^c(\Im a_k^c)^2\}\Re\mathbf{R_k^c} - 2\{(\Im a_k^c)^3 + (\Re a_k^c)^2\Im a_k^c\}\Im\mathbf{R_k^c} - 2\omega^2\{(\Re a_k^c)(\Re\mathbf{R_k^c}) - (\Im a_k^c)(\Im\mathbf{R_k^c})\}}{((\Re a_k^c)^2 + (\Im a_k^c)^2 - \omega^2)^2 + (2\omega\Re a_k^c)^2}$$
$$+ j\frac{-2\omega\{(\Re a_k^c)^2 - (\Im a_k^c)^2 + \omega^2\}\Re\mathbf{R_k^c} - 4\omega(\Re a_k^c)(\Im a_k^c)\Im\mathbf{R_k^c}}{((\Re a_k^c)^2 + (\Im a_k^c)^2 - \omega^2)^2 + (2\omega\Re a_k^c)^2} \tag{13}$$

$$\Re\hat{H}_k^c(j\omega) \succeq 0 \implies \frac{-2\{(\Re a_k^c)^3 + \Re a_k^c(\Im a_k^c)^2\}\Re\mathbf{R_k^c} - 2\{(\Im a_k^c)^3 + (\Re a_k^c)^2\Im a_k^c\}\Im\mathbf{R_k^c} - 2\omega^2\{(\Re a_k^c)(\Re\mathbf{R_k^c}) - (\Im a_k^c)(\Im\mathbf{R_k^c})\}}{((\Re a_k^c)^2 + (\Im a_k^c)^2 - \omega^2)^2 + (2\omega\Re a_k^c)^2} \succeq 0 \ \forall\omega, k = 1,...,\kappa_c \tag{14}$$

In order to obtain positive realness condition on $\hat{H}_k^c(j\omega)$ we rationalize (12) to form (13). The resulting condition for $\Re\hat{H}_k^c(j\omega) \succeq 0$ is given in (14)

3.4.3 Direct Term Matrix

Since D is a constant real symmetric matrix, we require D to be a positive semidefinite matrix, i.e.

$$D \succeq 0$$

3.5 The Constrained Minimization Problem

We combine all the constraints derived earlier and formulate a constrained minimization problem as follows:

$$\begin{aligned}
&\underset{\hat{H}\equiv\{\mathbf{R_k},a_k,\mathbf{D},\mathbf{F}\}}{\text{minimize}} && \sum_i \left|H_i - \hat{H}(j\omega_i)\right|^2 \\
&\text{subject to} && a_k^r < 0 \ \forall k = 1,...,\kappa_r \\
&&& \Re a_k^c < 0 \ \forall k = 1,...,\kappa_c \\
&&& \Re\hat{H}_k^r(j\omega) \succeq 0 \ \forall\omega, k = 1,...,\kappa_r \\
&&& \Re\hat{H}_k^c(j\omega) \succeq 0 \ \forall\omega, k = 1,...,\kappa_c \\
&&& \mathbf{D} \succeq 0 \\
&\text{where} && \hat{H}(j\omega) = \sum_{k=1}^{\kappa_r}\hat{H}_k^r(j\omega) + \sum_{k=1}^{\kappa_c/2}\hat{H}_k^c(j\omega) + \mathbf{D} + j\omega\mathbf{F}
\end{aligned} \tag{15}$$

Here H_i are the given frequency response samples at frequencies ω_i; $\hat{H}_k^r$ and $\hat{H}_k^c$ are defined in (7) and (8) respectively; a_k^r and a_k^c denotes the real and complex poles respectively. The detailed expressions for $\Re\hat{H}_k^r(j\omega) \succeq 0$ and $\Re\hat{H}_k^c(j\omega) \succeq 0$ are described in (11) and (14) respectively.

4. IMPLEMENTATION

In this section we describe in detail the implementation of our passive multiport model identification procedure based on solving the constrained minimization framework developed in Section 3.

The optimization problem in (15) is non-convex because both the objective function and the constraints are non-convex. The non-convexity in (15) arises mainly because of the terms containing *products* and *ratios* between decision variables such as ratio of residue matrices, R_k, and poles, a_k, in the objective function, and product terms and ratios of R_k and a_k in the constraints.

Since the main cause of non-convexity in (15) is the coupling between R_k and a_k, it is natural to uncouple the identification of unknowns, namely R_k and a_k in order to convexify (15). We propose to solve the optimization problem in (15) in two steps. The first step consists of finding a set of stable poles a_k for the system. The second step is to find a passive multiport dynamical model for the system, given stable poles from step 1. In the following sections we describe how to solve the two steps.

4.1 Step 1: Identification of stable poles

Several efficient algorithms already exist for the identification of stable poles for multiport systems. Some of the stable pole identification approaches use optimization based techniques such as in [3]. Some schemes such as [7, 8] find the location of stable poles iteratively. Any one of these algorithms can be used as the first step of our algorithm, where we identify a common set of stable poles for all the transfer functions in the transfer matrix. As before, to enforce conjugate symmetry, the stable poles can either be real or be in the form of complex-conjugate pairs.

4.2 Step 2: Identification of Residue Matrices

In this section we formulate the convex optimization problem for the identification of residue matrices using the stable poles from step 1. We first revisit the conditions for passivity (11) (14) and later we shall develop the convex objective function.

4.2.1 Purely Real Pole-Residues

Let us consider the positive realness condition on the purely real pole residue term $H_k^r(j\omega)$ as in (11). The constraint (11) requires frequency dependent matrices to be positive semidefinite for all frequencies. This is in general very expensive to enforce. However, a careful observation of (11) reveals that the denominator, which is the only frequency dependent part in (11) is always a positive real number for all frequency. Hence we can ignore the positive denominator which leaves us enforcing $-a_k^r\mathbf{R_k^r} \succeq 0$. Now since we are already given stable poles (i.e. $a_k^r < 0$), the constraint in (11) reduces to enforcing positive semidefiniteness on $\mathbf{R_k^r}$.

$$\Re\hat{H}_k^r(j\omega) \succeq 0 \implies \mathbf{R_k^r} \succeq 0 \ \forall k = 1,...,\kappa_r \tag{16}$$

Such a constraint is convex and can be enforced extremely efficiently using SDP solvers [11].

4.2.2 Complex Conjugate Pole-Residues

In this section we reconsider the positive realness condition on the complex conjugate pole residue pair term $H_k^c(j\omega)$ as in (14). As before, a closer examination of the frequency dependent denominator in (14) reveals the fact that it is positive for all frequencies. Given that we have a fixed set of stable poles, and the denominator is always positive, we rewrite the constraint (14) only in terms of the variables i.e. ω and $\mathbf{R_k^c}$. Also we replace the constant expressions of $\Re a_k^c$ and $\Im a_k^c$ in (14) with generic constants c_i. We finally obtain the following equivalent condition

$$\begin{aligned}
&\Re\hat{H}_k^c(j\omega) \succeq 0 \implies \\
&(c_1\Re\mathbf{R_k^c} + c_2\Im\mathbf{R_k^c}) + \omega^2(c_3\Re\mathbf{R_k^c} + c_4\Im\mathbf{R_k^c})\} \succeq 0 \ \forall\omega, k = 1,...,\kappa_c
\end{aligned} \tag{17}$$

The problem is however still not solved since the condition in (17) is frequency dependent.

LEMMA 4.1. *Let $X_1, X_2 \in \mathbb{S}^T$ and $\omega \in [0,\infty)$, where $\mathbb{S}^T$ is the set of symmetric $T \times T$ matrices, then*

$$X_1 + \omega^2 X_2 \succeq 0 \forall\omega \Leftrightarrow X_1 \succeq 0, X_2 \succeq 0 \tag{18}$$

PROOF. Direction $\Rightarrow$
Given $X_1 + \omega^2 X_2 \succeq 0$ we consider the following limits:

$$\begin{aligned}
&\lim_{\omega\to 0}(X_1 + \omega^2 X_2) \succeq 0 \implies X_1 \succeq 0 \\
&\lim_{\omega\to\infty}(X_1 + \omega^2 X_2) \succeq 0 \implies X_2 \succeq 0
\end{aligned} \tag{19}$$

Direction $\Leftarrow$ follows from the fact that non-negative weighted sum of positive semidefinite matrices is positive semidefinite. $\square$

We define

$$x_k^1 = c_1 \Re\mathbf{R_k^c} + c_2 \Im\mathbf{R_k^c}$$
$$x_k^2 = c_3 \Re\mathbf{R_k^c} + c_4 \Im\mathbf{R_k^c}, \qquad (20)$$

and apply Lemma 4.1 to the constraint defined in (17) which results into

$$\Re\hat{H}_k^c(j\omega) \succeq 0 \implies x_k^1 \succeq 0, x_k^2 \succeq 0 \; \forall k = 1, ..., \kappa_c \qquad (21)$$

Since x_k^1, x_k^2 are linear combinations of the unknown matrices, $\Im\mathbf{R_k^c}$ & $\Im\mathbf{R_k^c}$ the constraint (21) is a semidefinite convex constraint and thus can be enforced very efficiently.

4.2.3 Convex Optimization to Find Residue Matrices

In this section we summarize the final convex optimization identifying the residue matrices which correspond to to passive $H(j\omega)$, given stable poles a_k.

$$\begin{aligned}
\underset{\mathbf{R_k^r}, \mathbf{R_k^c}, \mathbf{D}, \mathbf{F}}{\text{minimize}} \quad & \sum_i \left| \Re H_i - \Re\hat{H}(j\omega_i) \right|^2 + \sum_i \left| \Im H_i - \Im\hat{H}(j\omega_i) \right|^2 \\
\text{subject to} \quad & \mathbf{R_k^r} \succeq 0 \; \forall k = 1, ..., \kappa_r \\
& c_1 \Re\mathbf{R_k^c} + c_2 \Im\mathbf{R_k^c} \succeq 0 \; \forall k = 1, ..., \kappa_c \\
& c_3 \Re\mathbf{R_k^c} + c_4 \Im\mathbf{R_k^c} \succeq 0 \; \forall k = 1, ..., \kappa_c \\
& \mathbf{D} \succeq 0 \\
\text{where} \quad & \hat{H}(j\omega) = \sum_{k=1}^{\kappa_r} \hat{H}_k^r(j\omega) + \sum_{k=1}^{\kappa_c/2} \hat{H}_k^c(j\omega) + \mathbf{D} + j\omega\mathbf{F}
\end{aligned} \qquad (22)$$

This final problem (22) is convex, since the objective function is a summation of L_2 norms. All the constraints in (22) are linear matrix inequalities. This convex optimization problem is a special case of semidefinite programming, requiring only few frequency independent matrices to be positive semidefinite. This problem formulation is extremely fast to solve, compared to other convex formulations [3, 4] where the unknown matrices are frequency dependent.

4.3 Circuit Synthesis

From circuits perspective, the algorithm identifies a collection of low-pass, band-pass, high-pass and all-pass passive filter networks. These passive blocks can readily be synthesized into an equivalent passive circuit networks and can be interfaced with commercial circuit simulators by either generating a spice-like netlist or by using Verilog-A. Alternatively we can develop equivalent state space realizations for our passive multiport models, for example, a Jordan-canonical form can be obtained as described in [8] and then diagonalized.

4.4 The Complete Algorithm

In this section we present the algorithmic description of the complete framework in Algorithm 1. This algorithm minimizes a cost function based on L_2 norm subject to linear matrix inequalities. Such a formulation can be solved very efficiently and is guaranteed to converge to global minimum. However the fact that this algorithm provides analytical expressions to enforce passivity in a highly efficient manner has enormous potential such as in future extensions to parameterized passive multiport models; or to include designers constraints such as matching qualify factor.

Algorithm 1 Complete Passive Multiport Model Identification

Input: The set of frequency response samples $\{H_i, \omega_i\}$, the number of poles N

Output: Passive model $\hat{H}(j\omega)$

1: Find the stable system with N poles a_k
2: Solve the optimization problem (22) for $\mathbf{R}_k$
3: Construct the model in pole/residue form as in (4)
4: Synthesize the equivalent passive circuit and generate the corresponding netlist or verilogA model file

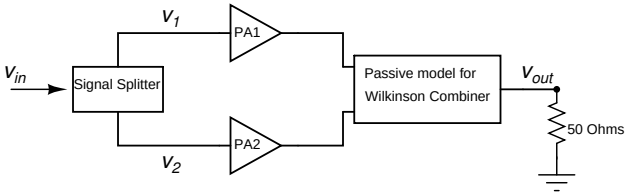

Figure 1: Block diagram of the LINC power amplifier architecture as simulated inside the circuit

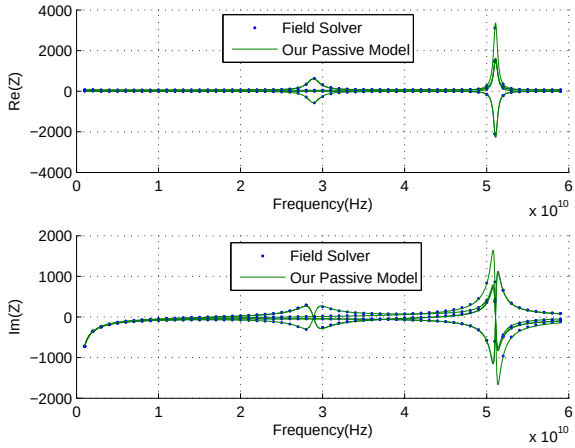

Figure 2: Comparing real and imaginary part of the impedance parameters from field solver (dots) and our passive model (solid lines). The mismatch, defined by (24)**,** $e_{i,k}(\omega) < 0.7\% \; \forall i, k, \omega \in [2, 60] GHz$

5. EXAMPLES

In this section we shall present modeling examples of various multiport passive structures. All examples are implemented in Matlab and run on a laptop with Intel Core2Duo processor with 2.1GHz clock, 3GB of main memory, and running windows 7. We have also posted free open source software implementing this algorithm online at [12].

5.1 Wilkinson Combiner in a LINC Amplifier

In this section we shall present an example illustrating the usefulness of our proposed methodology on modeling and simulating a LINC (*LI*near amplification with *N*onlinear *C*omponents) power amplifier. The architecture, as described in Figure 1, consists of a signal splitter, two power amplifiers, and a wilkinson type power combiner. This architecture is designed to operate at $40GHz$. *PA*1 and *PA*2 are class B amplifiers designed in $130nm$ SiGe process using BJTs. The wilkinson combiner is designed on alumina substrate with characteristic impedance of 50Ω and operating frequency of $40GHz$.

Input, v_{in}, to this architecture is a $64-QAM$ signal. The signal splitter decomposes the input *QAM* signal into two phase modulated fixed amplitude signals. Let $v_{in} = V_{in}\angle\phi$ be the input signal; $v_1 = V_0\angle\phi_1$ and $v_2 = V_0\angle\phi_2$ be the two signals generated by the splitter then,

$$v_{in} = v_1 + v_2, \qquad V_{in}\angle\phi = V_0\angle\phi_1 + V_0\angle\phi_2 \qquad (23)$$

The splitted signals are amplified by individual nonlinear power amplifiers. The outputs of these two power amplifiers are added using a wilkinson type power combiner. This 3-port wilkinson combiner, is simulated inside a full wave public domain field solver [13] available at [14]. Using the frequency response samples generated by the field solver, a closed form state space model of order $m = 30$ is identified using our passive modeling algorithm. To demonstrate the accuracy of this model in frequency domain Figure 2 compares the impedance parameters from field solver (dots) and frequency

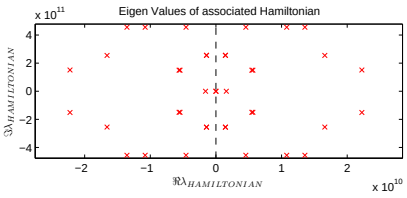

Figure 3: Plotting the zoomed-in eigen values of the associated hamiltonian matrix for the identified model of wilkinson combiner

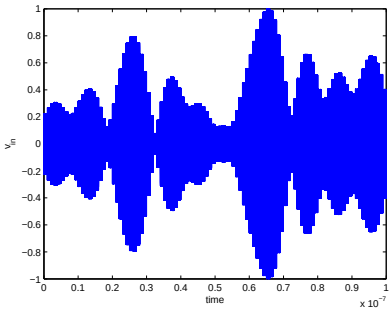

Figure 4: Ideal normalized 64-QAM input voltage v_{in}

response of our identified passive model (solid lines). The modeling error $e_{i,k}(\omega)$, defined by (24), was less than 0.7% for all i,k in the bandwidth of interest between $2-60GHz$

$$e_{i,k}(\omega) = \frac{|H_{i,k}(j\omega) - \hat{H}_{i,k}(j\omega)|}{\max_{i,k,\omega} |H_{i,k}(j\omega)|} \qquad (24)$$

The algorithm took only 2*seconds* to generate the entire model, whereas for the same order and simular accuracy the algorithm described in [3] took 83*seconds* giving us a speed-up of $40\times$.

A model is passive if there are no purely imaginary eigen values of the associated Hamiltonian matrix. Figure 3 is a zoomed-in plot of the eigen values of the associated hamiltonian matrix for the identified model. It is clear that the model passes the passivity test since there are no purely imaginary eigen values.

Finally, the overall amplifier architecture is simulated inside a circuit simulator after connecting the linear model for the combiner with the rest of the circuit components including the nonlinear amplifiers, as shown in Figure 1. Practically speaking, as verified in Figures 4 and 5, the passive nature of the identified model for the wilkinson combiner guarantee that transient simulations for the overall architecture converge and the final output signal v_{out} is also a $64-QAM$ signal similar to the input v_{in}.

5.2 Power Distribution Grid

The second example we present is a power & ground distribu-

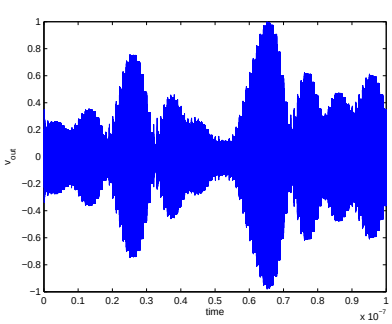

Figure 5: Normalized output voltage v_{out} generated by transient simulation of the overall architecture in Figure 1

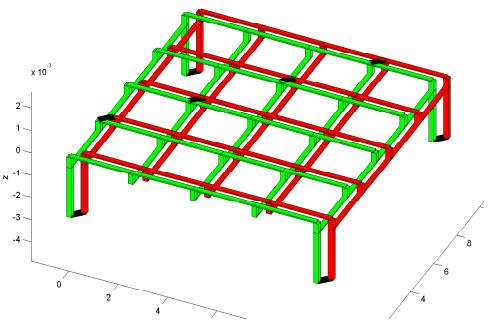

Figure 6: 3D layout of the distribution grid (not to scale) showing Vdd (red or dark grey) and Gnd (green or light grey) lines. Black strips represent location of ports

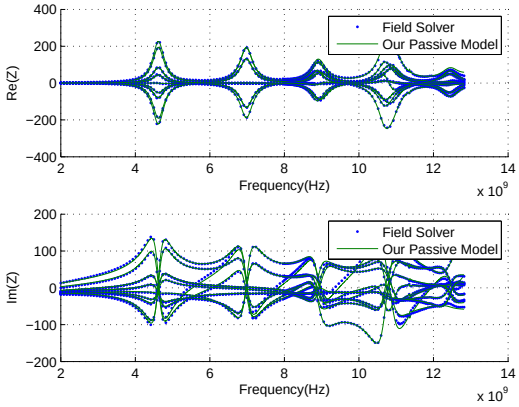

Figure 7: Comparing real part and imaginary of impedance from our passive model (solid line) and from field solver (dots) for power distribution grid

tion grid used in systems on chip or on package. The 3D layout for this power grid is shown in Figure 6, and is composed of Vdd (red or dark grey) and *Gnd* (green or light grey) segments placed along both x and y axes. External connections given by solder balls in a flip chip technology, are modeled with bond wires running vertically. This structure was simulated using 52390 unknowns in the full wave mixed potential integral equation (MPIE) solver, FastMaxwell [13], to obtain frequency response samples up to 12 GHz. The multiport simulation was arranged by placing eight ports: four at the grid corners and four inside the grid. Ports are illustrated in Figure 6 as black strips.

For this example our proposed algorithm identified an 8×8 passive transfer matrix of order $m = 160$ in 74*seconds*, whereas the algorithm in [3] ran out of memory for similar configuration and did not generate the model. To demonstrate the accuracy, Figure 7 compares the real and imaginary impedance respectively of our reduced model with the field solver data. Although the models are passive by construction, the passive nature was verified by the absence of purely imaginary eigen values of the associated hamiltonian matrix.

5.3 On-chip RF Inductors

The third example we shall discuss is a collection of 4 RF inductors on the same chip or package that are used in the design of multichannel receivers. The layout is shown in Figure 8. The structure has four ports in total, configured at the input of each inductor. This structure was simulated using 10356 unknowns in the full wave field solver, FastMaxwell [13] which captures substrate using a Green function complex image method.

For this example a 4×4 passive transfer matrix of order $m = 92$ was identified. The algorithm took 72*seconds* to identify the pas-

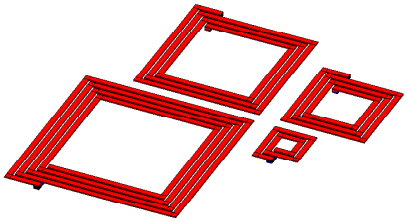

Figure 8: 3D layout of the RF inductors (wire widths not to scale)

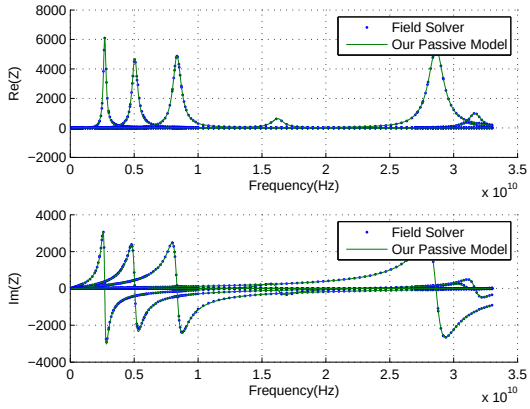

Figure 9: Comparing real part and imaginary of impedance from our passive model (solid line) and from field solver (dots) for the RF inductors

sive model, compared to the algorithm in [3] which ran out of memory for similar configuration. Figure 9 shows impedance parameters both from the field solver and from our identified model. The passive nature of this model was verified by the absence of pure imaginary eigen values of the associated hamiltonian matrix.

6. CONCLUSION

In this paper we have proposed a new semidefinite programming based algorithm to solve the original nonlinear and non-convex problem to identify passive multiport models. The identified models, because of the passive nature of construction, can be readily synthesized into equivalent circuits and hence can be interfaced with commercial simulators easily. The theory is supported by modeling and simulation of various multiport structures.Using same configuration, for simpler structures we were able to get a speed-up of 40× over [3] while for moderately large problems we were able to converge with in a reasonable amount of time whereas approaches such as [3] ran out of resources and did not generate the model.

7. ACKNOWLEDGEMENTS

Support for this project was provided by SRC, FCRP-IFC and DARPA. Mr. Mahmood gratefully acknowledges the support of Irwin Mark Jacobs and Joan Klein Jacobs Presidential Fellowship.

APPENDIX

A. CONJUGATE SYMMETRY

The condition requires $\overline{\hat{H}(\overline{j\omega})} = \hat{H}(j\omega)$. We show that the $\hat{H}(j\omega)$, as in (5) satisfies this constraint.

$$\hat{H}(\overline{j\omega}) =$$

$$\sum_{k=1}^{\kappa_r} \frac{\mathbf{R_k^r}}{-j\omega - a_k^r} + \sum_{k=1}^{\kappa_c/2} \left\{ \frac{\Re\mathbf{R_k^c} + j\Im\mathbf{R_k^c}}{-j\omega - \Re a_k^c - j\Im a_k^c} + \frac{\Re\mathbf{R_k^c} - j\Im\mathbf{R_k^c}}{-j\omega - \Re a_k^c + j\Im a_k^c} \right\} + \mathbf{D} - j\omega\mathbf{F}$$

$$\Rightarrow \overline{\hat{H}(\overline{j\omega})} =$$

$$\sum_{k=1}^{\kappa_r} \frac{\mathbf{R_k^r}}{j\omega - a_k^r} + \sum_{k=1}^{\kappa_c/2} \left\{ \frac{\Re\mathbf{R_k^c} - j\Im\mathbf{R_k^c}}{j\omega - \Re a_k^c + j\Im a_k^c} + \frac{\Re\mathbf{R_k^c} + j\Im\mathbf{R_k^c}}{j\omega - \Re a_k^c - j\Im a_k^c} \right\} + \mathbf{D} + j\omega\mathbf{F}$$

$$= \hat{H}(j\omega)$$

B. REFERENCES

[1] Jorge J. Moré. The levenberg-marquardt algorithm: Implementation and theory. In *Numerical Analysis*, Lecture Notes in Mathematics, pages 105–116. Springer Berlin / Heidelberg, 1978.

[2] Carlos P. Coelho, Joel R. Phillips, and L. Miguel Silveira. A convex programming approach to positive real rational approximation. In *Proc. of IEEE/ACM International Conference on Computer Aided-Design*, pages 245–251, San Jose, CA, November 2001.

[3] K. C. Sou, A. Megretski, and L. Daniel. A quasi-convex optimization approach to parameterized model order reduction. *IEEE Trans. on Computer-Aided Design of Integrated Circuits and Systems*, 27(3), Mach 2008.

[4] Z. Mahmood, B. Bond, T. Moselhy, A. Megretski, and L. Daniel. Passive reduced order modeling of multiport interconnects via semidefinite programming. In *Proc. of the Design, Automation and Test in Europe (DATE)*, Dresden, Germany, March 2010.

[5] S. Grivet-Talocia. Passivity enforcement via perturbation of hamiltonian matrices. *Circuits and Systems I: Regular Papers, IEEE Transactions on*, 51(9):1755–1769, Sept. 2004.

[6] B. Gustavsen. Fast passivity enforcement for pole-residue models by perturbation of residue matrix eigenvalues. *IEEE Trans. on Power Delivery*, 23(4), Oct. 2008.

[7] B. Gustavsen and A. Semlyen. Rational approximation of frequency domain responses by vector fitting. *IEEE Trans. on Power Delivery*, 14(3), Jul 1999.

[8] R. Achar and M.S. Nakhla. Simulation of high-speed interconnects. *Proceedings of the IEEE*, 89(5):693 –728, may 2001.

[9] J. Morsey and A.C. Cangellaris. Prime: passive realization of interconnect models from measured data. In *Electrical Performance of Electronic Packaging, 2001*, pages 47 –50, 2001.

[10] Sung-Hwan Min and M. Swaminathan. Construction of broadband passive macromodels from frequency data for simulation of distributed interconnect networks. *Electromagnetic Compatibility, IEEE Transactions on*, 46(4):544 – 558, nov. 2004.

[11] `http://sedumi.ie.lehigh.edu/`.

[12] `http://http://web.mit.edu/zohaib/www/`.

[13] T. Moselhy, Xin Hu, and L. Daniel. pfft in fastmaxwell: A fast impedance extraction solver for 3d conductor structures over substrate. In *Proc. of Design, Automation and Test in Europe Conference, 2007. DATE '07*, pages 1–6, April 2007.

[14] `http://www.rle.mit.edu/cpg/research_codes.htm`.